JOURNAL OF VIROLOGY, Feb. 2007, p. 2056–2064 Vol. 81, No. 4
0022-538X/07/$08.00+0 doi:10.1128/JVI.01911-06

Synergistic Attenuation of Vesicular Stomatitis Virus by Combination of Specific G Gene Truncations and N Gene Translocations▽

David K. Clarke,* Farooq Nasar, Margaret Lee, J. Erik Johnson, Kevin Wright, Priscilla Calderon, Min Guo, Robert Natuk, David Cooper, R. Michael Hendry, and Stephen A. Udem†

Wyeth Vaccines Discovery Research, 401 N. Middletown Road, Pearl River, New York 10965

Received 1 September 2006/Accepted 23 November 2006

A variety of rational approaches to attenuate growth and virulence of vesicular stomatitis virus (VSV) have been described previously. These include gene shuffling, truncation of the cytoplasmic tail of the G protein, and generation of noncytopathic M gene mutants. When separately introduced into recombinant VSV (rVSV), these mutations gave rise to viruses distinguished from their "wild-type" progenitor by diminished reproductive capacity in cell culture and/or reduced cytopathology and decreased pathogenicity in vivo. However, histopathology data from an exploratory nonhuman primate neurovirulence study indicated that some of these attenuated viruses could still cause significant levels of neurological injury. In this study, additional attenuated rVSV variants were generated by combination of the above-named three distinct classes of mutation. The resulting combination mutants were characterized by plaque size and growth kinetics in cell culture, and virulence was assessed by determination of the intracranial (IC) 50% lethal dose (LD_{50}) in mice. Compared to virus having only one type of attenuating mutation, all of the mutation combinations examined gave rise to virus with smaller plaque phenotypes, delayed growth kinetics, and 10- to 500-fold-lower peak titers in cell culture. A similar pattern of attenuation was also observed following IC inoculation of mice, where differences in LD_{50} of many orders of magnitude between viruses containing one and two types of attenuating mutation were sometimes seen. The results show synergistic rather than cumulative increases in attenuation and demonstrate a new approach to the attenuation of VSV and possibly other viruses.

Vesicular stomatitis virus (VSV) is a member of the *Vesiculovirus* genus of the family *Rhabdoviridae*. The negative-sense virus genome is 11,162 nucleotides long and contains five genes in the order 3′ N-P-M-G-L 5′, encoding the five major viral proteins (1, 3). The bullet-shaped VSV particle (160 nm by 80 nm) contains a ribonucleoprotein core (nucleocapsid) composed of genomic RNA closely associated with N protein and a RNA polymerase composed of a complex of L and P proteins enveloped in a host cell-derived plasma membrane (4, 18, 19, 44, 53, 56). Following uptake of the virus particle by susceptible cells, nucleocapsid and viral RNA polymerase are released into the cytoplasm and viral mRNA transcription ensues. A 3′-5′ gradient of viral mRNA transcription leads to abundant N protein expression and successively decreasing levels of P, M, G, and L proteins (1, 3, 15, 19, 27, 57). This gene expression gradient provides virus proteins in a suitable ratio for subsequent viral genome replication and assembly of mature virus particles. Virus replication in cell culture is rapid, and virus progeny are detectable 5 to 6 h postinfection.

Since the initial recovery of infectious recombinant VSV (rVSV) from genomic cDNA (39, 61), effort has been directed towards the development of rVSV as a vaccine vector targeting a variety of different human pathogens, including human immunodeficiency virus type 1 (HIV-1) (25, 31–34, 48–51). The major advantages of rVSV vaccine vectors and their immunogenicity and protective efficacy in animal models have been described in detail previously (12). However, VSV is both neurotropic and neurovirulent in mice (54, 58, 60) and can cause neurological disease when injected directly into the brain of cows and horses (24). The original rVSV Indiana serotype vector ($rVSV_{IN}$) developed by J. Rose and colleagues was less pathogenic following intranasal inoculation in mice than the cell culture-adapted virus from which it was derived, but the neurovirulence (NV) potential of this vector following direct intracranial (IC) inoculation was not known. To address this question, an exploratory nonhuman primate (NHP) NV study based on the methodology used for NV testing of mumps vaccine seed lots was carried out. In that pilot study, wild-type (wt) VSV_{IN} and $rVSV_{IN}$ caused clinical signs of severe neurological disease following intrathalamic inoculation of animals; two additional rVSV vectors expressing the HIV-1 Gag protein did not cause any clinical signs of disease, but histological examination of the central nervous system (CNS) in these animals revealed evidence of necrotic and inflammatory lesions (30). These findings indicated that $rVSV_{IN}$ vectors would require further attenuation before being considered suitable for clinical evaluation.

When it became possible to recover infectious VSV from genomic cDNA (39, 61), directed approaches to study rVSV attenuation were adopted. One attenuation strategy known as gene shuffling involves rearranging the natural gene order of VSV, which alters normal levels of gene expression (2, 60). Viruses modified by gene rearrangement often grow poorly in vitro and are typically less virulent in vivo (21–23, 42, 60).

A different attenuation strategy involves truncation of the

* Corresponding author. Mailing address: Department of Vaccines Discovery Research, Wyeth, 401 N. Middletown Road, Bldg. 180/267, Pearl River, NY 10965. Phone: (845) 602-3465. Fax: (845) 602-4941. E-mail: clarked3@wyeth.com.

† Present address: IAVI, 110 William Street, Floor 27, New York, NY 10038-3901.

▽ Published ahead of print on 6 December 2006.

29-amino-acid cytoplasmic tail (CT) region of the virus G protein (50, 55). Viruses with shortened CTs have slower growth rates, reach lower peak titers in vitro, and are less pathogenic in mice than unaltered viruses (49). Because N gene shuffles and G protein CT truncations involve gene translocations and deletion of part of the G gene, respectively, mutants generated by these strategies have a stable attenuation phenotype-genotype (23, 55).

A third attenuation strategy relies on nucleotide substitutions within the M gene that ablate expression of two in-frame overlapping polypeptides initiated downstream from the M protein translation start codon (29). Viruses that do not express these polypeptides demonstrate reduced cytopathology in a variety of cell lines and are highly attenuated in mice. Consequently, mutants that do not express these polypeptides have been called noncytopathic M mutants (M_{NCP}).

In this study, we sought to explore and define strategies that would allow step-wise increases in $rVSV_{IN}$ vector attenuation to levels beyond those previously described, thereby increasing the range of attenuated vectors from which to generate an ideal $rVSV_{IN}$–HIV-1 vaccine vector for future clinical evaluation. To achieve this we combined G protein CT truncations with either N gene shuffles or M_{NCP} gene mutations. Growth characteristics of the resulting $rVSV_{IN}$ combination mutants were studied in vitro, and their neurovirulence was assessed in a mouse IC 50% lethal dose (LD_{50}) model to determine degree and relative order of vector attenuation.

MATERIALS AND METHODS

Cells and virus. Vero and baby hamster kidney (BHK) cell lines were obtained from the American Type Culture Collection and propagated under conditions of 37°C and 5% CO_2 in Dulbecco's modified Eagle's medium containing 10% fetal bovine serum, sodium pyruvate (20 mM), and gentamicin (50 μg/ml). The tissue culture-adapted San Juan strain of the VSV Indiana serotype (VSV_{IN}), a recombinant form of VSV_{IN} ($rVSV_{IN}$) (39), $rVSV_{IN}$ expressing HIV-1 Gag protein ($rVSV_{IN}$ gag5), and two attenuated forms of $rVSV_{IN}$ gag5 ($rVSV_{IN}$CT1 gag5 and $rVSV_{IN}$CT9 gag5) were kindly provided by J. Rose (Yale University, New Haven, CT). A modified form of vaccinia virus Ankara (MVA) that expressed bacteriophage T7 RNA polymerase (MVA-T7) (62) was obtained from Bernard Moss (National Institutes of Health, Bethesda, Maryland) and further modified to express T7 RNA polymerase under the control of an early transcription promoter (38).

Virus propagation, purification, and titration. Virus was routinely amplified on BHK cell monolayers and titrated on Vero cell monolayers. For virus amplification BHK cells were infected at a multiplicity of infection (MOI) of 0.001 to 0.05 PFU/cell. Virus inoculum was adsorbed for 15 min at room temperature (RT) followed by 30 min at 37°C. Additional growth medium was then added, and cells were incubated at 37°C until they became rounded and detached from the flask. Infected cell supernatant was clarified by centrifugation for 10 min at 3,000 × *g*. The virus suspension was then flash frozen in an ethanol-dry ice bath and stored at −80°C prior to titration. Where necessary, virus was further purified from infected cell supernatant by centrifugation through 10% (wt/vol) sucrose in 1× phosphate-buffered saline (PBS). Briefly, ~20 ml of clarified cell supernatant was underlaid with 12 to 15 ml of 10% (wt/vol) sucrose in a Beckmann Ultraclear tube followed by centrifugation at 28,000 rpm in a Beckmann SW-28 rotor for 1.5 h at 4°C. Following centrifugation, supernatant was aspirated, the virus pellet was resuspended in PBS, and the virus suspension was flash frozen and stored at −80°C prior to plaque assay.

For virus titration by plaque assay, freshly confluent Vero cell monolayers in six-well plates were infected with 0.1-ml aliquots from serial 10-fold dilutions of rVSV in growth medium. An additional 0.4 ml of medium was added to each well to prevent cell desiccation, and virus was adsorbed for 15 min at RT followed by 30 min at 37°C. The virus inoculum was then removed, and cell monolayers were overlaid with 3 ml of 0.8% (wt/vol) agarose (SeaPlaque; Cambrex Bio Science Rockland, Inc., Rockland, ME) in growth medium. After 10 min at RT to allow the agarose to solidify, cells were incubated at 37°C in 5% CO_2 for 1 to 4 days for plaque development. The agarose overlay was then removed, monolayers were rinsed once with 2 ml of PBS, and cells were stained and fixed in 0.5 ml of 70% methanol containing 2% crystal violet for 5 min at RT. Plaques were counted after removal of excess stain under running water.

Generation of attenuated $rVSV_{IN}$ genome cDNAs. The generation of both CT1 and CT9 mutants has been previously described in detail (49, 55). The corresponding rVSV genomic cDNAs were generously provided by J. Rose (Yale University, New Haven, CT) and were used in the derivation of the combination mutants described below.

A method for gene translocation within $rVSV_{IN}$ genomic cDNA has been described in detail previously (2, 60). A different method of N gene translocation was used in this study. Briefly, the N gene was first deleted from $rVSV_{IN}$ genomic cDNA by replacing the natural BsaAI-XbaI genome fragment (Fig. 1) with a DNA fragment that was generated by in vitro ligation of two PCR products, one stretching from the BsaAI site in the plasmid vector to the exact 3′ end of the virus leader sequence (positive sense) and the other spanning the region from the transcription start signal of the P gene to the downstream XbaI site. Precise ligation of DNA containing the virus leader sequence, with DNA containing the exact 3′ end of the P gene, was achieved by addition of BsmBI sites to PCR primers. The N gene was then reinserted into the ΔN genome cDNA between the P and M genes (N2), between the M and G genes (N3), and between the G and L genes (N4) by use of a similar approach. For generation of the N2 genome cDNA, a PCR product spanning the entire N gene and 3′ CT intergenic dinucleotide was ligated to flanking PCR fragments in vitro; one DNA fragment stretched from the unique XbaI site to the 3′ end of the P gene and contained the P/M intergenic dinucleotide GT. A second DNA fragment spanned the entire M gene to the unique MluI site in the G gene. Addition of BsmBI sites to the 3′ and 5′ ends of the P and M gene fragments, respectively, and to 3′ and 5′ ends of the N gene fragment allowed all three DNA fragments to be ligated in vitro and then cloned into the XbaI and MluI sites of the ΔN genome cDNA. The N3 cDNA genome was constructed in a similar fashion. A PCR fragment spanning the region from the unique XbaI site in the P gene to the end of the M gene, including the 3′ CT intergenic dinucleotide, was ligated to a PCR fragment spanning the entire N gene, a 3′ CT intergenic dinucleotide, and the first 32 nucleotides of the G gene containing the unique MluI site. Both DNAs were ligated through BsmBI sites at the 3′ end of the P/M fragment and the 5′ end of the N gene fragment. This DNA fragment was then cloned into the unique XbaI and MluI sites of the ΔN cDNA genome. For generation of the N4 genome cDNA, a PCR product spanning the entire N gene was joined with flanking PCR products, one stretching from the unique MluI site to the end of the G gene, including the 3′ CT intergenic dinucleotide, and the other containing the G/L intergenic dinucleotide CT and the region from the 5′ end of the L gene to the unique HpaI site. All three fragments were joined by the addition of BsmBI sites to the 3′ and 5′ ends of the G and L gene fragments, respectively, and to the 3′ and 5′ ends of the N gene DNA fragment. The resulting contiguous DNA fragment was then cloned into the MluI and HpaI sites of the ΔN cDNA genome.

A plasmid cDNA containing the M_{NCP} gene in the $rVSV_{IN}$ backbone was generously provided by Michael Whitt (University of Tennessee, Nashville) (29). The M_{NCP} gag5 and M_{NCP}CT1 gag5 vectors were generated by cloning a DNA fragment that spanned the mutant M_{NCP} gene and part of the P gene into the unique XbaI-MluI sites of $rVSV_{IN}$ cDNAs (generously provided by J. Rose, Yale University, New Haven, CT) containing either the HIV-1 Gag gene inserted between the G and L genes ($rVSV_{IN}$ gag5) or the HIV-1 Gag gene inserted between a truncated (CT1) form of the G gene and the L gene ($rVSV_{IN}$CT1 gag5).

Four N gene shuffle-CT combination mutants (N2CT9, N2CT1, N3CT9, and N3CT1) were generated by swapping the G genes from the N2 and N3 cDNAs with the CT1 and CT9 truncated forms of the G gene via unique flanking MluI and HpaI sites.

Recovery of $rVSV_{IN}$ from cDNA. Infectious virus was recovered from genomic cDNA following transfection of BHK cells with a mixture of plasmids expressing VSV N, P, and L proteins and full-length positive-sense genomic RNA, all under the control of the bacteriophage T7 RNA polymerase transcription promoter (39). For transfection, 95% to 100% confluent BHK cell monolayers in six-well dishes were incubated for 4 h in 3% CO_2 at 32°C in 4.5 ml/well of fresh growth medium. Meanwhile, a plasmid DNA-$CaPO_4$ precipitate was prepared for each cell monolayer by mixing 2 to 4 μg of plasmid containing full-length genomic cDNA, 1.0 μg of N plasmid, 0.5 μg of P plasmid, 0.15 μg of L plasmid, 25 μl of $CaCl_2$ (2.5 M), and water to achieve a 250-μl final volume. The DNA-$CaPO_4$ precipitate was then formed by dropwise addition of 250 μl of 2× BBS (280 mM NaCl, 50 mM BES, 1.5 mM Na_2HPO_4, pH 6.95 to 6.98) with gentle vortexing. The mixture was incubated at RT for 20 min to allow precipitate formation and then added dropwise to cells with gentle swirling. To provide a source of T7 RNA

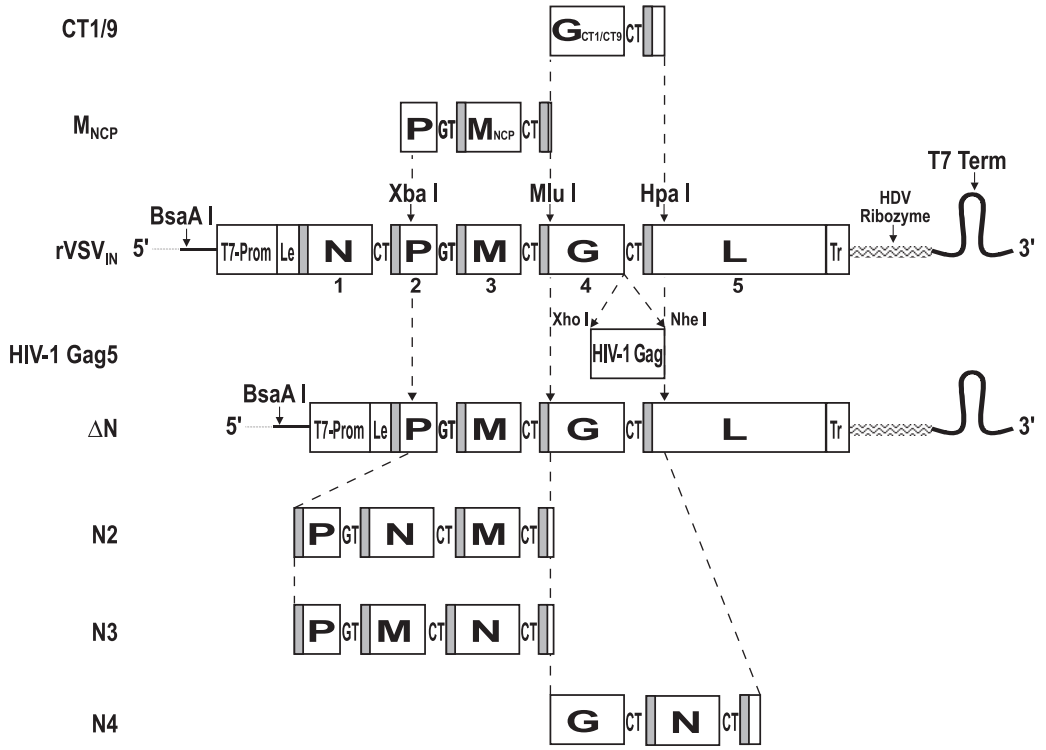

FIG. 1. Construction of $rVSV_{IN}$ mutant cDNA. The BsaAI, XbaI, MluI, and HpaI endonuclease sites used for construction of N gene shuffles and insertion of G genes containing CT truncations and M_{NCP} mutations are indicated with arrows. Virus leader (Le), trailer (Tr), GT, and CT intergenic dinucleotides and transcriptional start signals (shaded boxes) at the beginning of each gene are shown. Synthesis of positive-sense genomic RNA was under control of the T7 RNA polymerase transcription promoter (T7-Prom) and was terminated by a T7 transcription terminator (T7 Term). Hepatitis delta virus ribozyme (HDV Ribozyme) was used to generate the precise viral 3′ end on the positive-sense genomic RNA transcript.

polymerase, MVA-T7-GK16 (38) was then added to each well at an MOI of 3 to 4 PFU/cell along with 20 μg/ml cytosine arabinoside to inhibit amplification of MVA-T7. Cells were then incubated at 32°C in 3% CO_2 for 3 h followed by a 2-h heat shock at 43°C in 3% CO_2 (43). Following heat shock, cells were incubated at 32°C in 3% CO_2 for 18 to 24 h. Transfection medium was then replaced with 2 ml of fresh growth medium containing cytosine arabinoside, and cells were further incubated at 37°C in 5% CO_2 for 48 to 72 h. Transfected cells were then scraped into suspension, gently pipetted repeatedly to reduce cell clumping, and transferred to 95% to 100% confluent Vero cell monolayers in six-well dishes. The following day, cocultures were supplemented with 1 ml of fresh growth medium and incubation was continued for a further 3 to 5 days, during which time VSV cytopathic effect (CPE) became apparent. Rescued virus was then triple plaque purified and further amplified prior to in vitro and in vivo analysis.

In vitro growth studies. For comparison of $rVSV_{IN}$ mutant plaque sizes, plaque assays were performed in duplicate on replicate Vero cell monolayers as described above. For growth kinetics studies, replicate Vero cell monolayers in 25 cm^2 flasks were infected in duplicate at an MOI of 5 PFU/cell. Virus was adsorbed in 0.5 ml of growth medium for 15 min at RT followed by 30 min at 37°C with occasional rocking to prevent cell desiccation. After removal of the inoculum, monolayers were rinsed three times with 5 ml of PBS to remove unbound virus; 5 ml of growth medium was then added to each monolayer, and a 0.5-ml aliquot was immediately removed as a "time h 0" (T_0) sample and replaced with 0.5 ml of fresh medium. Incubation was continued at 37°C in 5% CO_2 for 48 to 72 h, and further samples were taken at T_3 to T_{48}. All samples were flash frozen in ethanol-dry ice and stored at −80°C for titration.

Mouse IC LD_{50} studies. Five-week-old female Swiss Webster mice (Taconic Laboratory Animals and Services, Germantown, NY) were anesthetized and injected IC with $\log_{10}$-fold dilutions of virus in 30 μl PBS (10 mice per dilution, with dilutions adjusted to range around the anticipated LD_{50}). Weight and health status were recorded daily for 2 weeks. Mice becoming either bilaterally paralyzed or showing significant signs of distress or severe illness were sacrificed and recorded as succumbing to VSV disease. The LD_{50} and the 50% paralyzing dose (PD_{50}) were determined by the method of Reed and Muench (45) based on the number of mice that became paralyzed. All animal care and procedures conformed to Institutional Animal Care and Use Committee guidelines. The facilities are fully accredited by the American Association for Accreditation of Laboratory Animal Care.

RESULTS

Recovery of attenuated $rVSV_{IN}$ vectors from genomic cDNA. The complete spectra of $rVSV_{IN}$ vectors recovered from genomic cDNA and subsequently used for in vitro and in vivo attenuation studies are shown in Fig. 2A. Attenuated $rVSV_{IN}$ mutants were generated using three different attenuation strategies and combinations thereof. In one strategy the N gene was translocated (shuffled) to the second, third, and fourth gene positions (N2, N3, and N4, respectively) in the $rVSV_{IN}$ genome. In another strategy, the G protein CT was truncated to either nine (CT9) amino acids or one (CT1) amino acid. A third attenuation strategy abolished expression of two overlapping polypeptides encoded within the M gene open reading frame, generating the M_{NCP} gag5 mutant containing the HIV-1 gag gene at position 5 in the genome. Both the CT9 and N4 mutants contain an additional "empty" transcriptional unit (TU) at the fifth position in the genome. This TU contains an XhoI-NheI cassette flanked by transcription start and stop signals to facilitate insertion and expression of foreign genes (50, 51). Because results from previous murine NV studies (60) and an exploratory NHP NV study (30) indicated that N gene shuffles and G protein CT truncations on their own might not

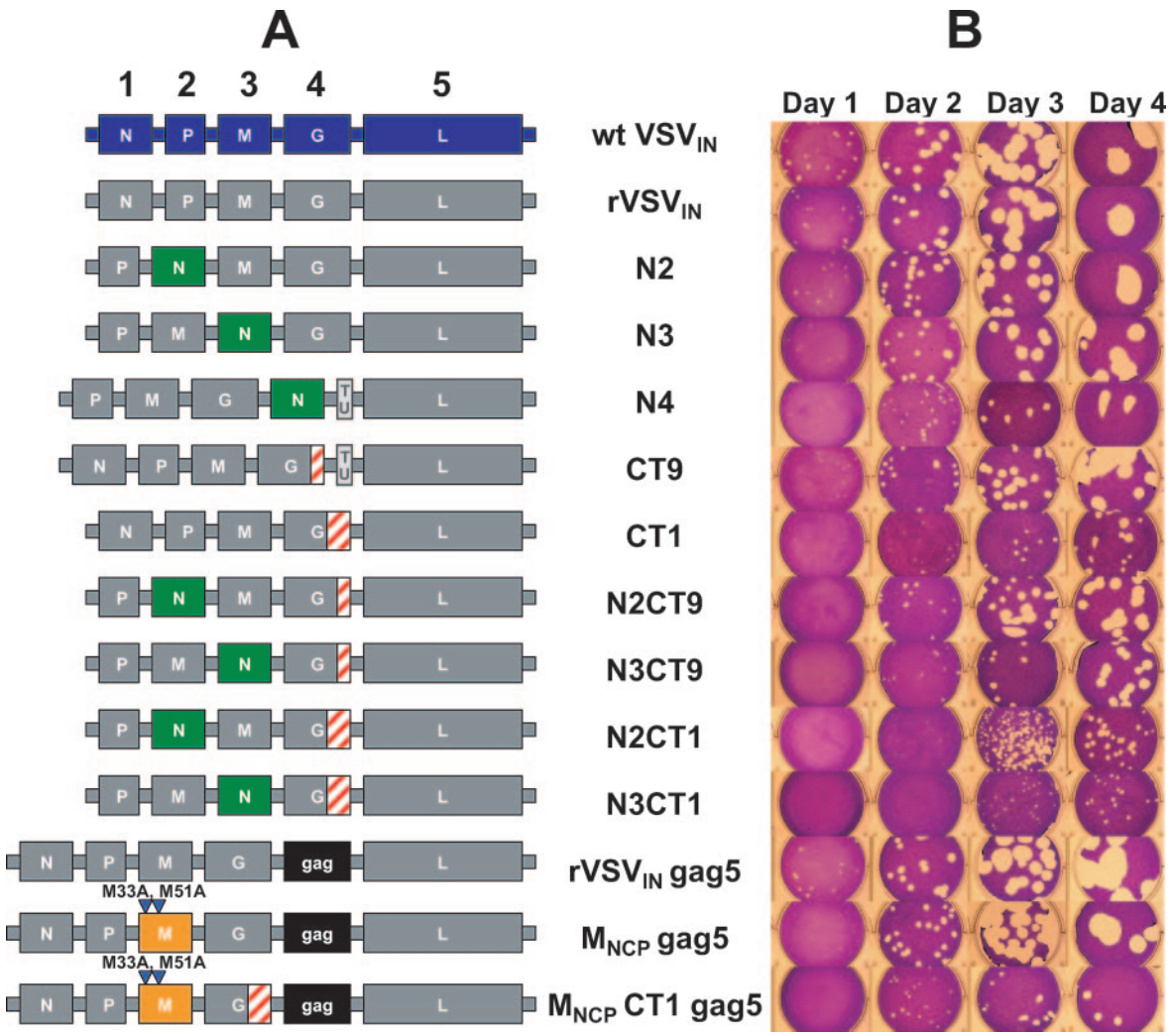

FIG. 2. Genetic organization of rVSV$_{IN}$ mutants and plaque size comparison. (A) Mutants were named to reflect genomic organization and attenuating mutations. The N gene shuffle mutants N2, N3, and N4 were named according to the position of the N gene relative to that of wt VSV$_{IN}$. The G protein CT truncation mutants CT1 and CT9 were named according to the number of amino acids retained in the cytoplasmic tail region of the G protein. Vectors containing noncytopathic M gene mutations (M33A and M51A [triangles]) were named M$_{NCP}$ mutants. Combination mutants were named N2CT1, N3CT1, N2CT9, N3CT9, and M$_{NCP}$CT1 to reflect contributing mutations. An additional empty TU containing transcription start and stop signals but no additional gene was present in N4 and CT9 mutants. The HIV-1 gag gene was present in the fifth position of virus genomes as indicated. (B) Representative plaques produced by wt VSV$_{IN}$ and rVSV$_{IN}$ variants following plaque assay on replicate Vero cell monolayers at 37°C for 1 to 4 days.

attenuate rVSV$_{IN}$ sufficiently for use as a vaccine vector in humans, these mutations were also combined in different configurations in an effort to produce more highly attenuated variants. Most double mutants were generated by combining N gene shuffles with G protein CT9 and CT1 truncations (shuffle-CT mutants), giving rise to N2CT9, N3CT9, N2CT1, and N3CT1 vectors; another double mutant containing the HIV-1 gag gene at position 5 in the genome was generated by combining the G protein CT1 truncation with the M$_{NCP}$ mutations (M$_{NCP}$ CT1 gag5). Even though it was anticipated that the mutant vectors would be more growth attenuated in vitro than the prototype rVSV$_{IN}$ vector developed by J. Rose and colleagues, all single and combination mutants were recoverable from cDNA.

Comparison of rVSV$_{IN}$ mutant plaque size. To gain a first impression on the relative attenuation levels of rVSV$_{IN}$ mutants, plaque sizes on Vero cell monolayers were compared at different times postinfection (Fig. 2B). From this analysis a number of trends emerged. Plaques produced by rVSV$_{IN}$ and wt VSV$_{IN}$ were almost the same size at all time points, indicating that rVSV$_{IN}$ growth was little more attenuated than wt VSV$_{IN}$ growth in cell culture. Virus containing only M$_{NCP}$-attenuating mutations (M$_{NCP}$ gag5) produced a delayed cell CPE, as previously observed (29), that resulted in very small plaques by day 1. At later time points, plaques were only slightly smaller than those made by rVSV$_{IN}$, indicating efficient growth and spread of this mutant in vitro. However, it should be noted that although M$_{NCP}$ plaques were similar in size to

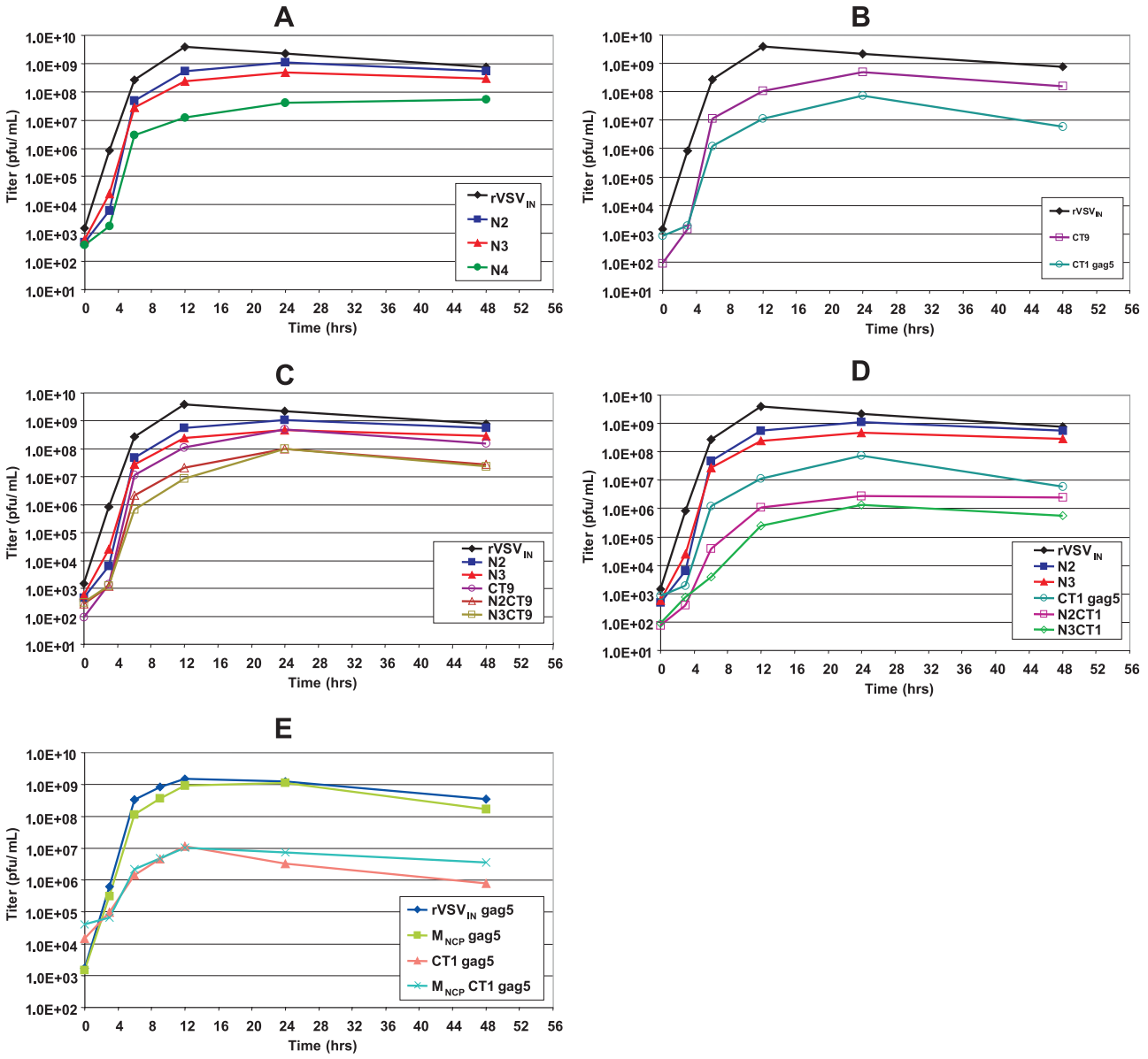

FIG. 3. Growth kinetics of $rVSV_{IN}$ mutants on Vero cell monolayers. Replicate Vero cell monolayers in 25 cm^2 flasks were infected in duplicate at an MOI of 5 PFU/cell. Infected-cell supernatants were collected at intervals postinfection and titrated on Vero cell monolayers. All datum points represent the average titers of samples taken from duplicate infections. Growth curves are shown for mutants containing N gene shuffles (A), CT truncations (B), N gene shuffle-CT truncation combinations (C and D), and M_{NCP} mutations (E).

those made by $rVSV_{IN}$ and $rVSV_{IN}$ gag5 at days 2 to 4, cells within the M_{NCP} gag5 plaques displayed a reduced CPE at all time points. The M_{NCP} CT1 gag5 combination mutant produced plaques that were much smaller than M_{NCP} gag5 plaques and similar in size to those produced by the CT1 virus, indicating that the CT1 truncation was the dominant attenuating mutation affecting virus growth and spread in vitro. Importantly, both CT and N gene shuffle mutants had plaque sizes commensurate with degrees of genetic alteration. For example, CT1 mutants produced smaller plaques than CT9 mutants, and there was a gradient of decreasing plaque size as the N gene was moved further away from the 3′ transcription promoter (N2 to N4), as previously reported (60). When N gene shuffle and CT mutations were combined, plaque size was decreased relative to the results seen with mutants having only one of the two mutations. For example, N2CT1 and N3CT1 produced plaques that were on average smaller than plaques produced by N2, N3, or CT1 mutants at all time intervals. This effect was also seen for N3CT9 but was less notable for N2CT9 except at day 1. Plaque sizes for N shuffle-CT combination mutants also varied incrementally with degree of genetic alteration, and a gradient of decreasing plaque size (N2CT9→N3CT9→N2CT1→N3CT1) was seen. Overall observations of plaque size indicated that the combination of N gene shuffles and CT truncations can attenuate virus incrementally and to a greater degree than either single form of mutation.

In vitro growth kinetics of $rVSV_{IN}$ mutants. We next performed a series of growth kinetic studies measuring the rate and extent of virus growth to further compare relative in vitro attenuation levels among $rVSV_{IN}$ mutants (Fig. 3). As shown in Fig. 3A, the rate of virus growth was reduced in relation to the position (N2 to N4) of the N gene, with a reduction in peak virus titer of 5-fold for N2, 10-fold for N3, and 100-fold for N4 compared to $rVSV_{IN}$ results. The CT9 and CT1 gag5 mutants (Fig. 3B) also had reduced growth rates and reached 10-fold and 100-fold-lower peak titer respectively than $rVSV_{IN}$, in general agreement with previous reports (49, 55). It should be noted that the addition of the HIV-1 gag gene between the G and L genes of $rVSV_{IN}$ did not significantly reduce growth of virus in cell culture and that the CT1 and CT1 gag5 mutants displayed almost identical growth kinetics in vitro (data not shown). More importantly, when N gene shuffles were combined with G protein CT truncations a series of virus mutants was generated that had reduced growth rates and a reduction in peak infectious particle production compared to virus containing either form of mutation alone (Fig. 3C and 3D). Overall, the growth kinetic studies indicated a gradient of increasing virus attenuation (N2CT9→N3CT9→N2CT1→N3CT1) identical to that observed in plaque size comparisons. In this combinatorial approach to virus attenuation, N3CT1 had 1,000-fold-lower peak virus titer than $rVSV_{IN}$ and 50- and 500-fold-lower peak titer than CT1 and N3 mutants, respectively (Fig. 3D). A separate series of growth kinetic studies were performed for the M_{NCP} mutants, as they were originally generated with the HIV-1 gag gene inserted between the G and L genes of the genome(s). As previously described, virus containing the M_{NCP} mutations replicated to a nearly normal peak titer in cell culture (Fig. 3E) but with a delayed onset of CPE in most cell types (29). Unlike the synergistic attenuation of virus growth seen with N gene-CT combination mutants, combining M_{NCP} mutations with the CT1 truncation did not significantly alter growth in cell culture compared to the results seen with the CT1 mutant alone, indicating that the CT1 mutation was the dominant attenuating mutation in vitro.

Assessment of $rVSV_{IN}$ vector neurovirulence in mice. Young mice are much more sensitive to infection with VSV following IC inoculation than following intranasal inoculation (54, 60). Moreover, unlike wt VSV_{IN}, attenuated $rVSV_{IN}$ mutants containing either cytoplasmic tail truncations (CT1 and CT9) or N gene shuffles (N2, N3, and N4) do not cause death following intranasal inoculation (25, 60). Therefore, to measure differences in virulence among the attenuated $rVSV_{IN}$ mutants, mice were inoculated IC, and the cumulative animal deaths, time until death, and frequency and severity of paralysis were measured. The LD_{50}s and the PD_{50}s were calculated based on the method of Reed and Muench and are shown in Fig. 4A. The time to death in animals receiving a lethal dose is shown in Fig. 4B.

Mice receiving wt VSV_{IN} reproducibly died 2 to 4 days postinoculation, and the LD_{50} was only 1 to 2 PFU. In agreement with plaque size comparisons and growth kinetics studies, $rVSV_{IN}$, with and without HIV gag inserted between the G and L genes, was only marginally more attenuated than wt VSV, with an LD_{50} of approximately 2 to 5 PFU and a slightly delayed onset of death at 2 to 5 days. Viruses containing either CT truncations or N gene shuffles alone were slightly more attenuated than $rVSV_{IN}$, with LD_{50} values of 12 to 21 PFU for CT9, CT1, N2, N3, and N4. Although the LD_{50}s of N2, N3, and N4 mutants were similar, there was a respective incremental increase in time to onset of death. However, a dramatic decrease in virulence was seen when the CT1 mutation was combined with N gene shuffles. Most notably, for N3CT1 the LD_{50} increased to $>10^5$ PFU compared to 15 PFU and 12 PFU for CT1 and N3 viruses, respectively, and the LD_{50} for N2CT1 was 1.1×10^4 PFU, demonstrating powerful synergistic attenuation of virulence for these combinations of mutations. Moreover, when animals died at higher doses, onset to death was delayed to 4 to 11 days postinoculation for N2CT1 and 6 to 14 days for N3CT1. To a lesser extent, and consistent with the order of attenuation observed in vitro, synergistic attenuation was also observed for N3CT9, with an LD_{50} of 524 PFU and delayed onset of death. As the least attenuated among the combination mutants in vitro, the LD_{50} dose for N2CT9 was very similar to the LD_{50}s for N2 and CT9; however, time to onset of death was delayed compared to that seen with the N2 and CT9 variants.

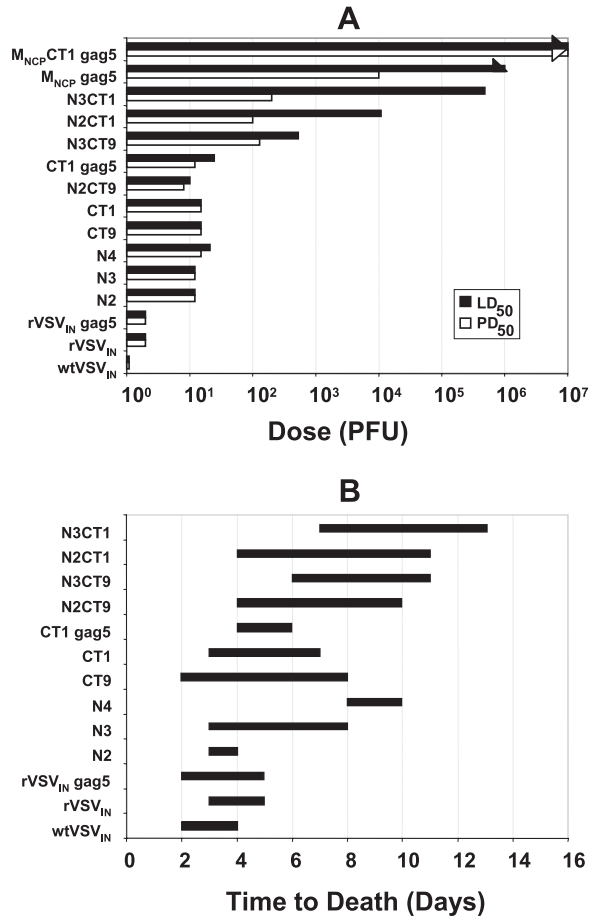

FIG. 4. Neurovirulence properties of $rVSV_{IN}$ mutants in mice following IC inoculation. In a series of experiments, 5-week-old Swiss Webster mice were inoculated IC with $\log_{10}$-fold dilutions of virus. Mice were monitored for 2 weeks for mortality and morbidity (paralysis). (A) The LD_{50} and PD_{50} values were determined by the method of Reed and Muench. (B) Time to death was recorded for mice in the group receiving the dose immediately above the determined LD_{50}. Arrowheads indicate results in which LD_{50} and PD_{50} were not achieved.

Many of the mice inoculated with the combination mutants, in particular, N3CT1 and N2CT1, displayed morbidity in the form of paresis and unilateral paralysis, from which they started to recover by week 3 postinfection, without mortality. Thus, the PD_{50}s for N3CT1 and N2CT1 were less than their respective LD_{50}s. Mice receiving the more virulent viruses died quickly without a measurable paralytic phase. Therefore, the PD_{50} and LD_{50} values for these viruses were recorded as being identical. Overall, the gradient of attenuation for the N gene shuffle-CT combination mutants observed in vivo was identical to that observed in vitro.

IC infection with M_{NCP} gag5 primarily caused some mild paralysis (PD_{50} of 10^4 PFU) but not death at up to the highest dose (10^6 PFU) tested, and an LD_{50} dose was not achieved. However, combining the M_{NCP} and CT1 mutations reduced the amount of paralysis compared to the results seen with M_{NCP} gag5 alone such that neither a LD_{50} nor a PD_{50} could be calculated for M_{NCP}CT1 gag5. The very high level of attenuation observed for the M_{NCP} gag and M_{NCP}CT1 gag5 mutants in vivo and the absence of a measurable LD_{50} for both mutants at input levels that were approaching a practical limit for M_{NCP}CT1 gag5 prevented any clear conclusions concerning the synergistic effect of combining the M_{NCP} and CT1 mutations. However, the M_{NCP} mutation was clearly the dominant attenuating mutation in vivo, while the CT1 mutation was clearly dominant in vitro.

DISCUSSION

An exploratory NV study of NHPs indicated that the $rVSV_{IN}$–HIV-1 vaccine vectors pioneered by J. Rose and colleagues retained significant levels of virulence and might be insufficiently attenuated for clinical evaluation (30). The present study was undertaken to investigate strategies for further attenuation of $rVSV_{IN}$ and to identify less-virulent variants that might be more suitable as vaccine vectors for HIV-1 and other pathogens.

Variants containing only a single form of attenuating mutation were more growth attenuated than the prototypic $rVSV_{IN}$ vector in vitro but, except for the M_{NCP} mutant, were still highly neurovirulent when tested in the murine IC NV model. Virus containing only the CT1 mutation also caused significant neuropathology in an exploratory NHP NV study (30). In an effort to further increase $rVSV_{IN}$ vector attenuation, CT truncations were combined with either N gene shuffles or M_{NCP} mutations. Most of the resulting combination mutants were more growth attenuated in vitro than vectors containing either single form of mutation. Growth kinetics studies showed that N2CT1 and N3CT1 reached approximately 500- to 1,000-fold-lower peak titers than $rVSV_{IN}$ and approximately 50- to 500-fold-lower peak titers than N2, N3, or CT1 mutants. Furthermore, the degree of vector attenuation could be altered incrementally depending on the pairing of specific N gene shuffle and CT mutations. For example, the N3CT1 mutant was more growth attenuated than N2CT1, which was more attenuated than N3CT9 and N2CT9 mutants. The gradient of increasing virus attenuation for these combination mutants was N2CT9→N3CT9→N2CT1→N3CT1. The same order of attenuation was also observed in vivo, but differences in attenuation between combination mutants and virus with only one type of attenuating mutation were even more dramatic. The N2, N3, CT9, and CT1 mutants still retained high levels of virulence following IC inoculation of mice (LD_{50}s of 12 to 21 PFU) consistent with previously published data for N gene shuffles (60). In contrast, N gene shuffle-CT combination mutants had incrementally increasing LD_{50}s ranging from 10 PFU for N2CT9 to $>10^5$ PFU for N3CT1. Specifically, attenuation synergy appeared to be greater when the CT1 truncation was combined with N2 and N3 gene shuffles.

The differences in relative attenuation between single and combination mutants observed in vitro probably reflect predominantly virus-specific growth attenuation factors. It is thought that the length of the CT tail of VSV G protein may affect the efficiency of virus budding from the cytoplasmic membrane of infected cells. Shorter CTs reduce the rate of particle formation and peak virus titer produced in vitro, possibly due to impaired CT interaction with viral core proteins (16, 28, 50, 55). The N gene shuffles attenuate virus by a different mechanism. During virus replication, N protein is essential for the encapsidation of nascent genomic RNA, and the resulting nucleocapsid structure is the functional template for mRNA transcription and further genome replication. When the N gene is translocated further away from the single 3′ transcription promoter, N protein expression decreases (60). Consequently, limiting N protein reduces the level of nucleocapsid available for transcription, replication, and subsequent incorporation into virus progeny. When transcription is reduced, all virus proteins are expressed less abundantly, placing additional constraints on the availability of all the components needed for assembly and morphogenesis of virus progeny. When both attenuation strategies are combined, not only are viral nucleocapsid and truncated G protein, along with other virus proteins, limiting for viral morphogenesis but impaired interactions between viral nucleocapsid core and the truncated G protein CT likely also further constrain the efficiency of mature particle formation. In vivo, innate and cellular immune responses are additionally superimposed on these growth-attenuating virus-specific factors and likely contribute to the level of attenuation observed in mice.

Innate immunity is usually rapidly induced in response to viral infection in the periphery and likely also plays an important role in controlling virus replication early (days 1 to 5) following IC inoculation of mice (7, 10, 46). Recently, a role for type I interferon has been proposed for control of attenuated but not pathogenic strains of rabies virus, a relative of VSV, following IC inoculation of mice (59), and it is possible that differences in virulence between attenuated and pathogenic strains of VSV can also be explained by differential stimulation of alpha/beta interferon in the CNS. VSV growth in the brain may also be controlled by the induction of nitric oxide, which can inhibit VSV replication in vitro and in neurons (5, 8, 11, 13, 35–37, 47). Acquired cellular immunity likely also plays an important role in killing some types of infected cells and clearance of virus in the CNS early (days 1 to 8) in the infection (11, 46). In contrast, the humoral immune response does not appear to have a significant role in the control and clearance of VSV from the CNS following direct IC inoculation of mice (7, 11).

In view of the host-specific responses to VSV infection of the CNS described above, it is possible that the more slowly rep-

licating, highly attenuated N gene shuffle-CT truncation combination mutants less efficiently down-regulate innate immune responses, leading to a more potent antiviral state (14). For example, reduced expression of the VSV M protein and associated polypeptides can diminish the efficiency of host cell protein shutoff, allowing more efficient induction of innate immune responses (9, 20, 26, 29). Since the N gene shuffle-CT truncation combination mutants also down-regulate viral gene expression, including the M gene, the innate immune response may be better able to control these viruses. Similar reasoning likely also explains the observed differences between in vitro and in vivo attenuation of M_{NCP} mutants described here. In vitro, the M_{NCP} gag5 and M_{NCP}CT1 gag5 mutants are not subject to innate immune responses, and peak titer is close to that of rVSV gag5 and CT1 gag5, respectively, indicating that the CT1 mutation was the dominant attenuating mutation in vitro. However, both M_{NCP} gag5 and M_{NCP}CT1 gag5 had highly attenuated phenotypes in mice, indicating that the M_{NCP} mutations were dominant in vivo, presumably due to the reduced ability of these viruses to interfere with innate immune responses.

In general, the mouse IC LD_{50} NV model proved to be highly sensitive and capable of discriminating changes in virulence within the range of attenuated rVSV vectors tested in this study. Rodent models have also been used to assess the NV potential of other virus vaccine vectors and some licensed live virus vaccines and vaccine candidates, including smallpox vaccine (40), some yellow fever virus vaccine strains (6), attenuated Venezuelan equine encephalitis virus (41), the Jeryl Lynn strain of mumps virus vaccine (52) and a modified measles virus vaccine strain (17). Interestingly, some of the more highly attenuated rVSV vectors described here produced less morbidity and mortality following IC inoculation than some of the licensed live virus vaccines. However, it should be emphasized that differences in virus biology and the natural susceptibility of different mouse strains to virus infection and replication make direct comparison of attenuation levels among different virus vaccines and candidate vaccines extremely difficult.

In summary, the net effect of combining specific N gene shuffles and G protein CT truncations was a measurable synergistic attenuation of $rVSV_{IN}$ growth in vitro and a dramatic reduction of virulence in the very sensitive mouse IC LD_{50} model. These findings suggest that combining mutations that interfere with viral morphogenesis by impairing interactions between structural proteins with mutations that lead to down-regulation of viral structural protein expression may be a useful general mechanism for synergistic attenuation of $rVSV_{IN}$ and other RNA and DNA viruses. Because of the potential of $rVSV_{IN}$ as a vaccine vector for HIV-1 and other human pathogens, experiments are now under way to confirm attenuation of the combination mutants in NHP NV studies and explore the immunogenicity of these highly attenuated $rVSV_{IN}$ vectors.

ACKNOWLEDGMENTS

We thank J. Rose for providing $rVSV_{IN}$, CT1, and CT9 cDNAs and Michael Whitt for providing cDNA encoding the M_{NCP} gene. We thank Chris Parks and Sue Witko for guidance on virus rescue.

This work was sponsored in part by an HIV-1 Vaccine Design and Development Team contract from the National Institutes of Health and the National Institute of Allergy and Infectious Diseases (HVDDT NO1-A1-25458).

REFERENCES

1. **Abraham, G., and A. K. Banerjee.** 1976. Sequential transcription of the genes of vesicular stomatitis virus. Proc. Natl. Acad. Sci. USA **73:**1504–1508.
2. **Ball, L. A., C. R. Pringle, B. Flanagan, V. P. Perepelitsa, and G. W. Wertz.** 1999. Phenotypic consequences of rearranging the P, M, and G genes of vesicular stomatitis virus. J. Virol. **73:**4705–4712.
3. **Ball, L. A., and C. N. White.** 1976. Order of transcription of genes of vesicular stomatitis virus. Proc. Natl. Acad. Sci. USA **73:**442–446.
4. **Baltimore, D., A. S. Huang, and M. Stampfer.** 1970. Ribonucleic acid synthesis of vesicular stomatitis virus. II. An RNA polymerase in the virion. Proc. Natl. Acad. Sci. USA **66:**572–576.
5. **Barna, M., T. Komatsu, and C. S. Reiss.** 1996. Activation of type III nitric oxide synthase in astrocytes following a neurotropic viral infection. Virology **223:**331–343.
6. **Barrett, A. D., and E. A. Gould.** 1986. Comparison of neurovirulence of different strains of yellow fever virus in mice. J. Gen. Virol. **67**(Pt. 4)**:**631–763.
7. **Bi, Z., M. Barna, T. Komatsu, and C. S. Reiss.** 1995. Vesicular stomatitis virus infection of the central nervous system activates both innate and acquired immunity. J. Virol. **69:**6466–6472.
8. **Bi, Z., and C. S. Reiss.** 1995. Inhibition of vesicular stomatitis virus infection by nitric oxide. J. Virol. **69:**2208–2213.
9. **Black, B. L., and D. S. Lyles.** 1992. Vesicular stomatitis virus matrix protein inhibits host cell-directed transcription of target genes in vivo. J. Virol. **66:**4058–4064.
10. **Chesler, D. A., and C. S. Reiss.** 2002. The role of IFN-gamma in immune responses to viral infections of the central nervous system. Cytokine Growth Factor Rev. **13:**441–454.
11. **Christian, A. Y., M. Barna, Z. Bi, and C. S. Reiss.** 1996. Host immune response to vesicular stomatitis virus infection of the central nervous system in C57BL/6 mice. Viral Immunol. **9:**195–205.
12. **Clarke, D. K., D. Cooper, M. A. Egan, R. M. Hendry, C. L. Parks, and S. A. Udem.** 2006. Recombinant vesicular stomatitis virus as an HIV-1 vaccine vector. Springer Semin. Immunopathol. **28:**239–253. (First published 15 September 2006; doi:10.1007/s00281-006-0042-3.)
13. **Colasanti, M., T. Persichini, G. Venturini, and P. Ascenzi.** 1999. *S*-Nitrosylation of viral proteins: molecular bases for antiviral effect of nitric oxide. IUBMB Life **48:**25–31.
14. **Conzelmann, K. K.** 2005. Transcriptional activation of alpha/beta interferon genes: interference by nonsegmented negative-strand RNA viruses. J. Virol. **79:**5241–5248.
15. **Davis, N. L., and G. W. Wertz.** 1982. Synthesis of vesicular stomatitis virus negative-strand RNA in vitro: dependence on viral protein synthesis. J. Virol. **41:**821–832.
16. **Dubovi, E. J., and R. R. Wagner.** 1977. Spatial relationships of the proteins of vesicular stomatitis virus: induction of reversible oligomers by cleavable protein cross-linkers and oxidation. J. Virol. **22:**500–509.
17. **Duprex, W. P., I. Duffy, S. McQuaid, L. Hamill, S. L. Cosby, M. A. Billeter, J. Schneider-Schaulies, V. ter Meulen, and B. K. Rima.** 1999. The H gene of rodent brain-adapted measles virus confers neurovirulence to the Edmonston vaccine strain. J. Virol. **73:**6916–6922.
18. **Emerson, S. U., and R. R. Wagner.** 1972. Dissociation and reconstitution of the transcriptase and template activities of vesicular stomatitis B and T virions. J. Virol. **10:**297–309.
19. **Emerson, S. U., and Y. Yu.** 1975. Both NS and L proteins are required for in vitro RNA synthesis by vesicular stomatitis virus. J. Virol. **15:**1348–1356.
20. **Ferran, M. C., and J. M. Lucas-Lenard.** 1997. The vesicular stomatitis virus matrix protein inhibits transcription from the human beta interferon promoter. J. Virol. **71:**371–377.
21. **Flanagan, E. B., L. A. Ball, and G. W. Wertz.** 2000. Moving the glycoprotein gene of vesicular stomatitis virus to promoter-proximal positions accelerates and enhances the protective immune response. J. Virol. **74:**7895–7902.
22. **Flanagan, E. B., T. R. Schoeb, and G. W. Wertz.** 2003. Vesicular stomatitis viruses with rearranged genomes have altered invasiveness and neuropathogenesis in mice. J. Virol. **77:**5740–5748.
23. **Flanagan, E. B., J. M. Zamparo, L. A. Ball, L. L. Rodriguez, and G. W. Wertz.** 2001. Rearrangement of the genes of vesicular stomatitis virus eliminates clinical disease in the natural host: new strategy for vaccine development. J. Virol. **75:**6107–6114.
24. **Frank, A. H., A. Appleby, and H. R. Seibold.** 1945. Experimental intracerebral infection of horses, cattle, and sheep with the virus of vesicular stomatitis. Am. J. Vet. Res. **6:**28–38.
25. **Haglund, K., J. Forman, H. G. Krausslich, and J. K. Rose.** 2000. Expression of human immunodeficiency virus type 1 Gag protein precursor and envelope proteins from a vesicular stomatitis virus recombinant: high-level production of virus-like particles containing HIV envelope. Virology **268:**112–121.
26. **Her, L. S., E. Lund, and J. E. Dahlberg.** 1997. Inhibition of Ran guanosine

triphosphatase-dependent nuclear transport by the matrix protein of vesicular stomatitis virus. Science **276:**1845–1848.
27. **Iverson, L. E., and J. K. Rose.** 1981. Localized attenuation and discontinuous synthesis during vesicular stomatitis virus transcription. Cell **23:**477–484.
28. **Jayakar, H. R., E. Jeetendra, and M. A. Whitt.** 2004. Rhabdovirus assembly and budding. Virus Res. **106:**117–132.
29. **Jayakar, H. R., and M. A. Whitt.** 2002. Identification of two additional translation products from the matrix (M) gene that contribute to vesicular stomatitis virus cytopathology. J. Virol. **76:**8011–8018.
30. **Johnson, J. E., F. Nasar, J. W. Coleman, R. E. Price, A. Javadian, K. Draper, M. Lee, P. A. Reilly, D. K. Clarke, R. M. Hendry, and S. A. Udem.** 9 November 2006, posting date. Neurovirulence properties of recombinant vesicular stomatitis virus vectors in non-human primates. Virology [Online.] doi:10.1016/J.Virol.2006.10.026.
31. **Jones, S. M., H. Feldmann, U. Stroher, J. B. Geisbert, L. Fernando, A. Grolla, H. D. Klenk, N. J. Sullivan, V. E. Volchkov, E. A. Fritz, K. M. Daddario, L. E. Hensley, P. B. Jahrling, and T. W. Geisbert.** 2005. Live attenuated recombinant vaccine protects nonhuman primates against Ebola and Marburg viruses. Nat. Med. **11:**786–790.
32. **Kahn, J. S., A. Roberts, C. Weibel, L. Buonocore, and J. K. Rose.** 2001. Replication-competent or attenuated, nonpropagating vesicular stomatitis viruses expressing respiratory syncytial virus (RSV) antigens protect mice against RSV challenge. J. Virol. **75:**11079–11087.
33. **Kahn, J. S., M. J. Schnell, L. Buonocore, and J. K. Rose.** 1999. Recombinant vesicular stomatitis virus expressing respiratory syncytial virus (RSV) glycoproteins: RSV fusion protein can mediate infection and cell fusion. Virology **254:**81–91.
34. **Kapadia, S. U., J. K. Rose, E. Lamirande, L. Vogel, K. Subbarao, and A. Roberts.** 2005. Long-term protection from SARS coronavirus infection conferred by a single immunization with an attenuated VSV-based vaccine. Virology **340:**174–182.
35. **Komatsu, T., Z. Bi, and C. S. Reiss.** 1996. Interferon-gamma induced type I nitric oxide synthase activity inhibits viral replication in neurons. J. Neuroimmunol. **68:**101–108.
36. **Komatsu, T., D. D. Ireland, N. Chen, and C. S. Reiss.** 1999. Neuronal expression of NOS-1 is required for host recovery from viral encephalitis. Virology **258:**389–395.
37. **Komatsu, T., D. D. Ireland, N. Chung, A. Dore, M. Yoder, and C. Shoshkes Reiss.** 1999. Regulation of the BBB during viral encephalitis: roles of IL-12 and NOS. Nitric Oxide **3:**327–339.
38. **Kovacs, G. R., C. L. Parks, N. Vasilakis, and S. A. Udem.** 2003. Enhanced genetic rescue of negative-strand RNA viruses: use of an MVA-T7 RNA polymerase vector and DNA replication inhibitors. J. Virol. Methods **111:** 29–36.
39. **Lawson, N. D., E. A. Stillman, M. A. Whitt, and J. K. Rose.** 1995. Recombinant vesicular stomatitis viruses from DNA. Proc. Natl. Acad. Sci. USA **92:**4477–4481.
40. **Li, Z., S. A. Rubin, R. E. Taffs, M. Merchlinsky, Z. Ye, and K. M. Carbone.** 2004. Mouse neurotoxicity test for vaccinia-based smallpox vaccines. Vaccine **22:**1486–1493.
41. **Ludwig, G. V., M. J. Turell, P. Vogel, J. P. Kondig, W. K. Kell, J. F. Smith, and W. D. Pratt.** 2001. Comparative neurovirulence of attenuated and non-attenuated strains of Venezuelan equine encephalitis virus in mice. Am. J. Trop. Med. Hyg. **64:**49–55.
42. **Martinez, I., L. L. Rodriguez, C. Jimenez, S. J. Pauszek, and G. W. Wertz.** 2003. Vesicular stomatitis virus glycoprotein is a determinant of pathogenesis in swine, a natural host. J. Virol. **77:**8039–8047.
43. **Parks, C. L., R. A. Lerch, P. Walpita, M. S. Sidhu, and S. A. Udem.** 1999. Enhanced measles virus cDNA rescue and gene expression after heat shock. J. Virol. **73:**3560–3566.
44. **Patton, J. T., N. L. Davis, and G. W. Wertz.** 1983. Cell-free synthesis and assembly of vesicular stomatitis virus nucleocapsids. J. Virol. **45:**155–164.
45. **Reed, E., and H. Muench.** 1938. A simple method of estimating fifty percent endpoints. Am. J. Hyg. **27:**493–497.
46. **Reiss, C. S., D. A. Chesler, J. Hodges, D. D. Ireland, and N. Chen.** 2002. Innate immune responses in viral encephalitis. Curr. Top. Microbiol. Immunol. **265:**63–94.
47. **Reiss, C. S., and T. Komatsu.** 1998. Does nitric oxide play a critical role in viral infections? J. Virol. **72:**4547–4551.
48. **Reuter, J. D., B. E. Vivas-Gonzalez, D. Gomez, J. H. Wilson, J. L. Brandsma, H. L. Greenstone, J. K. Rose, and A. Roberts.** 2002. Intranasal vaccination with a recombinant vesicular stomatitis virus expressing cottontail rabbit papillomavirus L1 protein provides complete protection against papillomavirus-induced disease. J. Virol. **76:**8900–8909.
49. **Roberts, A., L. Buonocore, R. Price, J. Forman, and J. K. Rose.** 1999. Attenuated vesicular stomatitis viruses as vaccine vectors. J. Virol. **73:**3723–3732.
50. **Roberts, A., E. Kretzschmar, A. S. Perkins, J. Forman, R. Price, L. Buonocore, Y. Kawaoka, and J. K. Rose.** 1998. Vaccination with a recombinant vesicular stomatitis virus expressing an influenza virus hemagglutinin provides complete protection from influenza virus challenge. J. Virol. **72:**4704–4711.
51. **Rose, N. F., P. A. Marx, A. Luckay, D. F. Nixon, W. J. Moretto, S. M. Donahoe, D. Montefiori, A. Roberts, L. Buonocore, and J. K. Rose.** 2001. An effective AIDS vaccine based on live attenuated vesicular stomatitis virus recombinants. Cell **106:**539–549.
52. **Rubin, S. A., M. Pletnikov, and K. M. Carbone.** 1998. Comparison of the neurovirulence of a vaccine and a wild-type mumps virus strain in the developing rat brain. J. Virol. **72:**8037–8042.
53. **Rubio, C., C. Kolakofsky, V. M. Hill, and D. F. Summers.** 1980. Replication and assembly of VSV nucleocapsids: protein association with RNPs and the effects of cycloheximide on replication. Virology **105:**123–135.
54. **Sabin, A., and P. Olitsky.** 1938. Influence of host factors on neuroinvasiveness of vesicular stomatitis virus. J. Exp. Med. **67:**201–227.
55. **Schnell, M. J., L. Buonocore, E. Boritz, H. P. Ghosh, R. Chernish, and J. K. Rose.** 1998. Requirement for a non-specific glycoprotein cytoplasmic domain sequence to drive efficient budding of vesicular stomatitis virus. EMBO J. **17:**1289–1296.
56. **Thomas, D., W. W. Newcomb, J. C. Brown, J. S. Wall, J. F. Hainfeld, B. L. Trus, and A. C. Steven.** 1985. Mass and molecular composition of vesicular stomatitis virus: a scanning transmission electron microscopy analysis. J. Virol. **54:**598–607.
57. **Villarreal, L. P., M. Breindl, and J. J. Holland.** 1976. Determination of molar ratios of vesicular stomatitis virus induced RNA species in BHK21 cells. Biochemistry **15:**1663–1667.
58. **Wagner, R. R.** 1974. Pathogenicity and Immunogenicity for Mice of Temperature-Sensitive Mutants of Vesicular Stomatitis Virus. Infect. Immun. **10:**309–315.
59. **Wang, Z. W., L. Sarmento, Y. Wang, X. Q. Li, V. Dhingra, T. Tseggai, B. Jiang, and Z. F. Fu.** 2005. Attenuated rabies virus activates, while pathogenic rabies virus evades, the host innate immune responses in the central nervous system. J. Virol. **79:**12554–12565.
60. **Wertz, G. W., V. P. Perepelitsa, and L. A. Ball.** 1998. Gene rearrangement attenuates expression and lethality of a nonsegmented negative strand RNA virus. Proc. Natl. Acad. Sci. USA **95:**3501–3506.
61. **Whelan, S. P., L. A. Ball, J. N. Barr, and G. T. Wertz.** 1995. Efficient recovery of infectious vesicular stomatitis virus entirely from cDNA clones. Proc. Natl. Acad. Sci. USA **92:**8388–8392.
62. **Wyatt, L. S., B. Moss, and S. Rozenblatt.** 1995. Replication-deficient vaccinia virus encoding bacteriophage T7 RNA polymerase for transient gene expression in mammalian cells. Virology **210:**202–205.